Practical and Accurate Calculations of Radio Emission from Extensive Air Showers

Washington Carvalho Jr.,[a,*] **Austin Cummings,**[b] **Andrew Ludwig**[c] **and Andres Romero-Wolf**[c]

[a]*IMAPP, Radboud University,*
Nijmegen, the Netherlands

[b]*Departments of Physics and Astronomy & Astrophysics, Institute for Gravitation and the Cosmos,*
Pennsylvania State University, University Park, PA 16802, USA

[c]*Jet Propulsion Laboratory, California Institute of Technology*
Pasadena, CA 91109, USA

E-mail: carvajr@gmail.com

We present a novel semi-analytical treatment of the radio emission of air showers that is able to reproduce the results of full ZHAireS simulations, in theory at a fraction of the computational cost. Traditionally, the contribution to the vector potential of every single particle track in the shower is calculated separately. Instead, in our approach we divide the air shower into 4-D spacetime volumes, so that the contribution of the volume needs to be calculated only once, based on the average particle track inside it. This almost amounts to a macroscopic treatment of the shower, but retaining the precision of the successful microscopic approach.

The size of the 4-D spacetime volumes is chosen so that the traditional vector potential expression can be further simplified, as many of its terms can be taken to be the same for the whole volume. Computationally expensive terms, such as the the effective refractive index from the track to the observer, can then be calculated only once, making it possible to obtain the precise radio emission at a fraction of the cost.

This approach also allows us to perform more precise calculations that would otherwise be too expensive to apply on a track-by-track basis. These could include a more detailed treatment of atmospheric effects for near horizontal showers and high altitude detectors, such as balloons and satellites.

---

*Speaker

1. Introduction

Ultra-high energy cosmic rays (UHECR) and high energy neutrinos provide a unique window into the observation of the most extreme events in the universe. UHECR and high energy neutrinos can be observed by measuring emission from secondaries formed by particle cascades following the interaction of the primary particles. Extensive Air Showers (EAS), or particle cascades in air, are of particular interest, as the cascade spatially develops over kilometers, making detection more probable. While many experiments measure UHECR induced EAS through the direct detection of secondary particles or their fluorescence and optical Cherenkov emission, we focus here on detection through the measurement of their radio emission.

The secondaries produced during the development of an EAS produce coherent radio emission through two mechanisms: geomagnetic and Askaryan emission. As the secondary particles within the EAS propagate, the electrons and positrons (which make up the bulk of the shower) are deflected from one another inside Earth's geomagnetic field, and on a macroscopic scale, represent a moving electric dipole which coherently emits radiation, referred to as geomagnetic emission. Geomagnetic emission is the dominant source of radio emission for EAS, and is highly dependent on the local magnetic field and the geometry of the shower. The propagating secondaries within the EAS also interact with the atmosphere, undergoing Compton, Moller, and Bhabha scattering and positron annihilation, leading to an overall negative charge excess. On a macroscopic scale, this excess represents a charge moving relativistically through the atmosphere, which generates a Cherenkov-like radio emission referred to as Askaryan emission.

Radio emission from EAS induced by cosmic rays has been observed by many different experiments in a variety of environments, and the measurement and reconstruction techniques are well understood. In recent years, there has been a growing interest in measuring the radio emission from upward going EAS sourced from ν_τ interactions in the Earth. The ANITA experiment has reported multiple events with this type of phenomenology: two steeply upwards going events observed by ANITA-I and ANITA-III [1, 2], and four near-horizon events observed by ANITA-IV [3]. A main science goal of the PUEO experiment is to follow-up on these events and better understand their characteristics [4].

The simulation of radio emission from EAS, both geomagnetic and Askaryan, is a matured topic, and has been critical in the design of current and next-generation radio experiments for UHECR and neutrino observation. One method of simulation, the microscopic approach, involves calculating and summing the vector potential produced by secondaries on track-by-track approach via equation 1, which does not presuppose any emission mechanism:

$$\mathbf{A}\left(\mathbf{x}, t\right) = \frac{\mu_0 q}{4\pi R}\mathbf{v}_\perp \frac{1}{|1 - n\left(h_{emit}\right)\boldsymbol{\beta}\cdot\mathbf{R}|}\Pi\left(t', t_1', t_2'\right) \tag{1}$$

Where R is the distance from the emitter to the observer, $\mathbf{v}_\perp$ is the projection of the particle velocity onto the plane perpendicular to the line of sight vector, $n\left(h_{emit}\right)$ is the index of refraction at the height of the emitter, and Π is a boxcar function that is equal to 1 between the start time, t_1',

and end time, t'_2, of the track, and 0 elsewhere.

While the microscopic method has great success in accurately modeling both the Askaryan and geomagnetic emission from EAS, one of the primary drawbacks is that it grows prohibitively slow and computationally expensive with increasing shower resolution (less thinning, or more particle tracks). Extremely large antenna arrays and long duration flights are envisioned for the future radio detection of UHECR and high energy neutrinos, thereby requiring extensive simulations of high-fidelity EAS from i) downward going cosmic rays ii) upwards going, neutrino-sourced secondaries iii) above the horizon cosmic rays.

Several methods attempt to make up for the shortcomings of the microscopic approach, but have their own pitfalls that can make them undesirable. Previous macroscopic modeling attempts are well parameterized for downward going cosmic ray induced EAS but fail to function in the geometries required for both upward going neutrino-sourced showers and cosmic rays from above the horizon [5]. The radiomorphing approach uses the emission from a reference shower to model the emission from an arbitrary shower and detector layout, sensibly scaling electric fields and time traces, treating the emitter as a point source at shower maximum $X_{\max}$ [6]. The results of the radio morphing approach closely reproduce the results of the microscopic approach in the case of downwards going cosmic rays for frequencies below 300 MHz, but diverge for higher frequencies, likely limited by the point-source approximation. The scalings presented by the radiomorphing approach are also not valid for upward going or above-the-horizon EAS geometries. A method is needed that emulates the speed of other macroscopic approaches while maintaining the accuracy of the microscopic approach.

2. Approach

The single track formalism calculation of the vector potential detailed in equation 1 can be generalized to a summation of currents in 4-dimensional spacetime via equation 2:

$$\mathbf{A}_i\left(\mathbf{x}, t\right) = \frac{\mu_0(Q\mathbf{v})_{i\mathrm{eff}\perp}}{4\pi R_i} \left| \frac{dt'_{i\mathrm{eff}}}{dt} \right|_{t'=t'_{ret}} \Pi\left(t', t'_{1\mathrm{eff}}, t'_{2\mathrm{eff}}\right) \tag{2}$$

where the effective quantities are given by:

$$(Q\mathbf{v})_{i\mathrm{eff}} = \frac{\sum_j w_{ij} q_{ij} \mathbf{v}_{ij} dt'_{ij}}{\sum_j dt'_{ij}}$$

$$(dt')_{i\mathrm{eff}} = |t'_{2\mathrm{eff}} - t'_{1\mathrm{eff}}| = \frac{\sum_j w_{ij} q_{ij} |v_{ij}| dt'_{ij}}{\sum_j w_{ij} q_{ij} |v_{ij}|}$$

This calculation amounts to almost a macroscopic treatment of the shower, in that many tracks are effectively averaged over, but retains the microscopic precision by treating the summed currents via equation 1. The advantage in performing this practical and accurate approach comes from having to calculate R and $\left|\frac{dt'}{dt}\right|$ once per each volumetric cell. Because each cell should contain
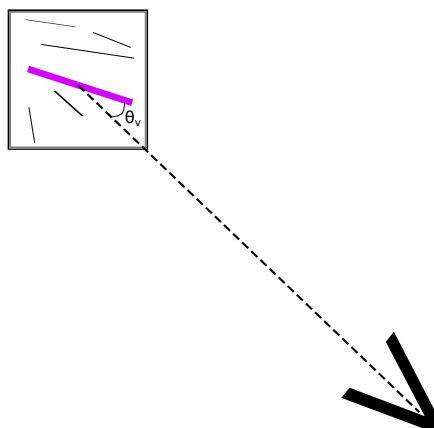
Figure 1: Simplified 2-D diagram of the practical and accurate calculation of radio emission concept. The black square represents a single bin within the EAS, while the thin black lines within the bin represent the individual current from secondary tracks, which added together form the effective current, shown by the thick purple line. The radiation at the detector is calculated using this effective current and the view angle, θ_v

many individual particle tracks, the computation time using this method should decrease by a factor corresponding to the average number of particle tracks contained within a 4-D cell. In particular, the calculation of $\left|\frac{dt'}{dt}\right|$ requires a calculation of the effective index of refraction along the path from the emitter to the receiver n_{eff} and can be very computationally expensive, requiring an integral along the line of sight in a non-uniform atmosphere. A simplified diagram of the practical and accurate radio calculation concept is shown in Figure 1.

2.1 Cell Size Optimization

The number of tracks that can be contained within a single 4-D cell (and thus, the efficiency of the practical and accurate approach described here) is restricted by the maximum volume of the cells. In the microscopic approach, to ignore higher order diffraction terms of emission, calculations performed on a single track are limited by the Fraunhofer approximation:

$$L < L_F = \frac{1}{\sin\theta}\sqrt{\frac{\lambda R}{2\pi}} \tag{3}$$

where L is track length, R is the distance from the center of the track to observer, λ is the radiation wavelength, and θ is the angle between the center of the track and the observer. For tracks with lengths L above the Fraunhofer limit, the view angle is not well defined and errors due to higher order terms in the phase approach $\pm\pi$. In the microscopic approach, tracks with $L > L_F$ are broken into smaller tracks which obey equation 3. We can consider an analogous approach regarding the practical and accurate method, whereby the 4-D cells have side lengths (L_F, L_F/c). Such cell dimensions represent the maximum size a cell should have to retain accuracy, and are sufficiently small such that many contributions to $\overrightarrow{A}$ can be averaged over the cell.

The maximum dimensions of the 4-D cells depend on both the wavelength of the emission and the distance from the cell to the observer, following equation 3. If constant cell sizes were to be
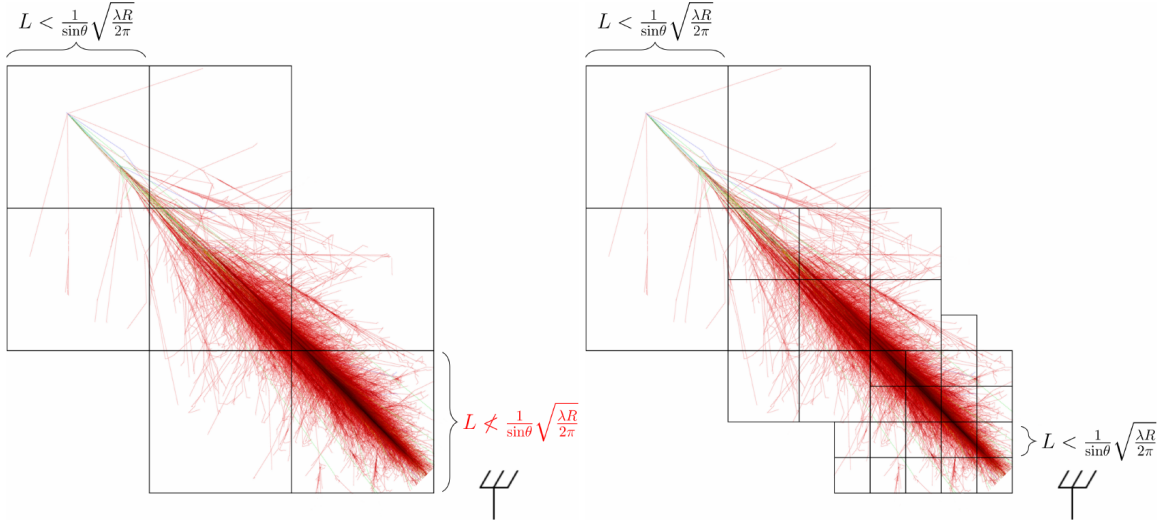
Figure 2: Diagram of the octree binning method of an air shower. Cells are initialized to be very large to capture as many particle tracks as possible. If the side length of a cell does not meet a minimum size set by the method (typically some multiple of the Fraunhofer approximation, shown in equation 3), it is subdivided into eight equal volumes, such that binning of the shower tracks takes place over unequal sized 4-D volumes. Subvolumes that do not contain tracks are ignored. Shower image taken from CORSIKA simulation [7].

used, they should be limited by their smallest cell, occurring when high frequencies are emitted near the observer. However, this strategy is not optimized, as cells further away from the observer are allowed to be significantly larger while obeying the Fraunhofer limit, thereby containing more tracks and reducing the computation time. We therefore consider an optimized, non-uniform cell sizing, hereby called octtree binning. In this approach, we first consider large cells of side length $(L, L/c)$ that cover the entirety of the shower, and define a minimum cell side length equal to AL_F, the maximum length which obeys the Fraunhofer approximation scaled by a factor A. The angular factor θ in equation 3 is preset to 60°, as currents with angles greater than this have negligible contributions to the vector potential. For any given 4-D cell, if the side length is less than the locally calculated AL_F, all side lengths of the cell are divided by two, resulting in eight new subvolumes. Any subvolumes that do not contain tracks are ignored in the final calculation. This strategy is repeated until all cells have side lengths that obey the condition $L < AL_F$. A 2-D diagram of the octree concept is shown in Figure 2, where the left panel represents the initialization of the binning, and the right panel represents the optimized binning.

3. Comparisons and Discussion

As a basic test of the practical and accurate approach, we calculate the radio emission of a downward going cosmic ray and compare the results against the microscopic method via the ZHAireS simulation package [8]. For this comparison, we consider an EAS induced by a 1 EeV proton primary with a zenith angle of 70°, and a particle thinning of 10^{-3}, observed at a position $P = [500 \text{ m}, 0 \text{ m}, 0 \text{ m}]$. For consistency between the two methods, the particle tracks passed to the practical and accurate method were the same ones generated in ZHAireS, simply without the

radio emission calculation. To demonstrate the effect of the cell sizes, we consider two scenarios: a maximum box size of L_F, and a maximum box size of $0.1L_F$, both accurate to 1 GHz frequencies, following the logic presented above.

Figure 3 shows a comparison between the microscopic approach via ZHAireS (in blue) and the practical and accurate approach (in orange) for a single cosmic ray induced EAS. The left column corresponds to simulation performed with the larger 4-D cell size, with side lengths L_F, while the right column corresponds to the cells with side length $0.1L_F$. The first row of Figure 3 shows the frequency spectra of the vector potential of the shower, while the second and third rows show, respectively, the full bandwidth and 30-80 MHz bandpass filtered time domain electric fields, calculated from the vector potential.
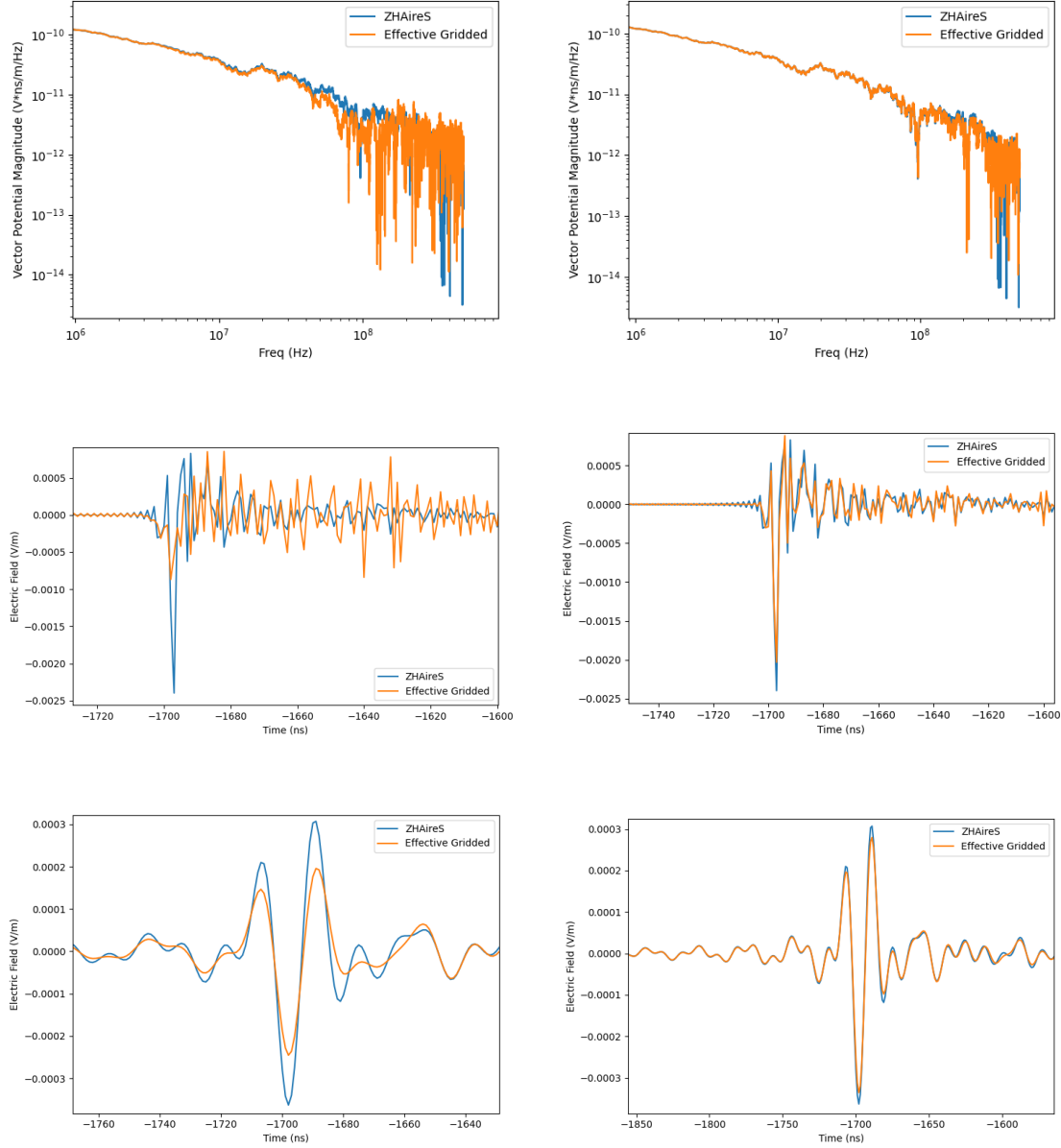
Figure 3 shows that the practical and accurate approach closely reproduces the radio emission calculated with ZHAireS. In particular, using cell side lengths of $0.1L_F$, even the full bandwidth time domain signals up to 500 MHz are well reproduced, improving on the results of the radio morphing approach. For larger cell sizes, low frequency behavior is still reasonably well approximated at the cost of poor high frequency behavior. This is due to the fact that at low frequencies, the Fraunhofer limit, and consequently, the cell sizes we have chosen, are not as strict, following equation 3. This indicates that for modelling radio experiments which target lower frequency bands (such as AERA [9] or BEACON [10]), the approach we have defined here can be somewhat relaxed, and cell sizes can be less optimized, allowing for fast computations.

4. Outlook

The practical and accurate 4-dimensional binning approach to the calculation of radio emission from EAS shows a significant amount of promise. For basic showers, the approach has shown to be able to reproduce the vector potential and electric field calculated using the microscopic, track-by-track method performed in ZHAireS. While the reduction in computation time using this approach over the microscopic approach is negligible for highly thinned showers (as presented in this work), it is expected that it will grow exponentially for reduced thinning (i.e. more realistic showers), where the number of individual tracks increases.

In the near future, this approach will be applied to consider the case of upwards going EAS sourced from neutrino interactions in the Earth. Previous simulations of these showers using ZHAireS have given rise to anomalous behavior in rarified atmosphere that needs to be verified. The macroscopic approach we have defined here allows for spherical propagation of radiation and may help to solve the discrepancy. In a similar vein, the difficulties involved in using the microscopic approach to calculate the emission from near-horizon cosmic rays may be significantly reduced, allowing for background event rate estimations for high altitude radio experiments.

This technique can also prove useful in studying the impact of atmospheric variations on the signal properties, particularly for upward going events. Whereas such a calculation using the microscopic approach is computationally exhaustive, and conventional macroscopic approaches fail,

Figure 3: Comparison of radio emission produced by a downward going cosmic ray induced EAS, as calculated with ZHAireS (blue) and the practical and accurate approach (orange). The left columns correspond to 4-D cells with a maximum side length L_F, the Fraunhofer limit, while the right columns correspond to maximum side lengths of $0.1L_F$. Both cell sizes assume a maximum frequency of 1 GHz. The first row shows the frequency spectra of the vector potential, while the second and third row show the full bandwidth and 30-80 MHz bandpass filtered time domain electric fields, respectively.

this approach reduces the complexity and the computation time while retaining the microscopic accuracy. In this work, we have only discussed the application to particle cascades produced in the atmosphere. However, the practical and accurate approach can also logically be extended to in-ice showers for ground arrays such as ARA, and RNO-G, where the near-field effects of a shower become relevant, and the ice density gradients are not trivial.

The practical and accurate approach to calculating radio emission of EAS presented in this work represents a complimentary approach to calculations via the microscopic approach and other available macroscopic approaches. Future studies will quantify the limits of this approach and highlight the benefits in significantly greater detail.

References

[1] P. W. Gorham *et al.*, "Characteristics of Four Upward-Pointing Cosmic-Ray-like Events Observed with ANITA," *Phys. Rev. Lett.*, vol. 117, p. 071101, 2016.

[2] P. W. Gorham *et al.*, "Observation of an Unusual Upward-going Cosmic-ray-like Event in the Third Flight of ANITA," *Phys. Rev. Lett.*, vol. 121, no. 16, p. 161102, 2018.

[3] P. W. Gorham *et al.*, "Unusual Near-Horizon Cosmic-Ray-like Events Observed by ANITA-IV," *Phys. Rev. Lett.*, vol. 126, no. 7, p. 071103, 2021.

[4] The PUEO Collaboration, "The payload for ultrahigh energy observations (PUEO): a white paper," *Journal of Instrumentation*, vol. 16, p. P08035, aug 2021.

[5] O. Scholten, T. N. G. Trinh, K. D. de Vries, and B. M. Hare, "Analytic calculation of radio emission from parametrized extensive air showers: A tool to extract shower parameters," *Phys. Rev. D*, vol. 97, p. 023005, Jan. 2018.

[6] A. Zilles, O. Martineau-Huynh, K. Kotera, M. Tueros, K. de Vries, W. Carvalho, V. Niess, N. Renault-Tinacci, and V. Decoene, "Radio morphing: towards a fast computation of the radio signal from air showers," *Astroparticle Physics*, vol. 114, pp. 10–21, jan 2020.

[7] D. Heck, J. Knapp, J. N. Capdevielle, G. Schatz, and T. Thouw, *CORSIKA: a Monte Carlo code to simulate extensive air showers.* 1998.

[8] J. Alvarez-Muñiz, W. R. Carvalho, and E. Zas, "Monte carlo simulations of radio pulses in atmospheric showers using ZHAireS," *Astroparticle Physics*, vol. 35, pp. 325–341, jan 2012.

[9] T. H. and, "Radio detection of cosmic rays with the auger engineering radio array," *EPJ Web of Conferences*, vol. 210, p. 05011, 2019.

[10] D. Southall *et al.*, "Design and Initial Performance of the Prototype for the BEACON Instrument for Detection of Ultrahigh Energy Particles," 2022.